Simulations for Planning Next-Generation Exoplanet Radial Velocity Surveys

Patrick D Newman[1], Peter Plavchan[1], Jennifer A. Burt[2], Johanna Teske[3], Eric E. Mamaje[2], Stephanie Leifer[4], B. Scott Gaudi[5], Garry Blackwood[2], Rhonda Morgan[2]
[1]George Mason University, [2]Jet Propulsion Laboratory, [3]Carnegie Institution for Science, [4]The Aerospace Corporation, [5]The Ohio State University

Abstract

Future direct imaging missions such as HabEx and LUVOIR aim to catalog and characterize Earth-mass analogs around nearby stars. The exoplanet yield of these missions will be dependent on the frequency of Earth-like planets, and potentially the a priori knowledge of which stars specifically host suitable planetary systems. Ground or space based radial velocity surveys can potentially perform the pre-selection of targets and assist in the optimization of observation times, as opposed to an uninformed direct imaging survey. In this paper, we present our framework for simulating future radial velocity surveys of nearby stars in support of direct imaging missions. We generate lists of exposure times, observation time-series, and radial velocity time-series given a direct imaging target list. We generate simulated surveys for a proposed set of telescopes and precise radial velocity spectrographs spanning a set of plausible global-network architectures that may be considered for next generation extremely precise radial velocity surveys. We also develop figures of merit for observation frequency and planet detection sensitivity, and compare these across architectures. From these, we draw conclusions, given our stated assumptions and caveats, to optimize the yield of future radial velocity surveys in support of direct imaging missions. We find that all of our considered surveys obtain sufficient numbers of precise observations to meet the minimum theoretical white noise detection sensitivity for Earth-mass habitable zone planets, with margin to explore systematic effects due to stellar activity and correlated noise.

Survey Targets, Goals, and Architectures

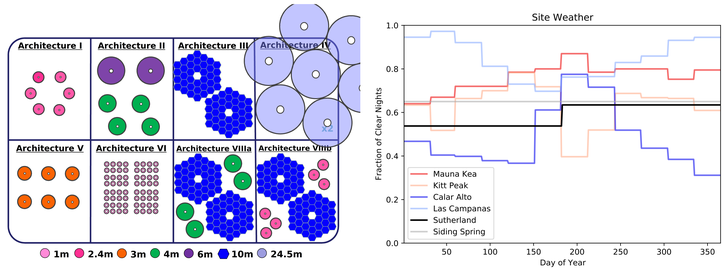

Figure: Left: General diagrams of different architecture(telescope/spectrograph combinations). Right: Nightly weather (as fraction of useable nights) at the sites considered for these surveys.

We took a list of 101 nearby ($\leq$ 15 pc) FGK stars that are considered both good direct imaging and RV targets, and split them into two mostly non-overlaping groups (51 north and 58 south). We performed simulated 10 year surveys on them across seven different architectures (telescope/instrument combinations) on six different sites (3 north, 3 south).

Architecture	I	IIa	IIb	V
Telescopes	6x2.4 m	2x6 m and 4x4 m	6x4 m	6x3 m
Collecting area by aperture	2.4 m = 4.2 m^2	4 m = 9.5 m^2; 6 m = 27 m^2	4 m = 9.5 m^2	3 m = 6.3 m^2
Time allocation	100%	100%	100%	100%
Wavelength coverage	380-930 nm	380 - 930 nm	380 - 930 nm	500-1700 nm
Spectral resolution	180 000	180 000	180 000	180 000
Total system efficiency	6%	6%	6%	7%
instrument noise floor	10 cm/s	5 cm/s	5 cm/s	10 cm/s
Required (peak) SNR/pix	300	300	300	300
Required RV precision	10 cm/s	10 cm/s	10 cm/s	10 cm/s
Observation cadence per star	1 / night	3 / night	3 / night	2 / telescope / night

Architecture	VI	VIIIa	VIIIb
Telescopes	6x arrays of 1 m	2x10 m and 4x 3.5 m	2x10 m and 6x2.4 m
Collecting area by aperture	0.61m^2 each; array is 9.5 m^2	10 m = 75 m^2; 3.5 m = 9.5 m^2 25% of 10 m; 100% of 3.5m	10 m = 75 m^2; 2.4 m = 4.2 m^2 25% of 10 m; 100% of 2.4 m
Time allocation	100%		
Wavelength coverage	500-800 nm	380-930 nm	380-930 nm
Spectral resolution	150 000	180 000	180 000
Total system efficiency	6%	6%	6%
instrument noise floor	10 cm/s	5 cm/s	5cm/s
Required (peak) SNR/pix	300	1000 for the 10 m; 300 for 3.5 m	1000 for the 10 m; 300 for 2.4 m
Required RV precision	10 cm/s	15 cm/s on 3.5 m; 5 cm/s on 10 m	15 cm/s on 2.4 m; 5 cm/s on 10 m
Observation cadence per star	1/night	1/week on 10 m; 1/night on 3.5 m	1/week on 10 m; 1/night on 2.4 m

Table: The seven architectures' facility and instrumental properties. Architectures not listed (III, IV, VII) were dropped from direct consideration in earlier simulations. Architectures with a/b variants have different sizes/numbers of telescopes, but identical instruments for each variant.

Code Description

Our survey code uses the MINERVA scheduler as a starting point, which we have modified for our simulations. It performs a physically motivated Monte Carlo simulation of an observing campaign, and includes a visualization script for the results. We take site location (latitude, longitude, altitude, weather), target properties (right ascension, declination, exposure time), survey duration, sun/moon position, and telescope properties (park position, slew speed, integration time, minimum altitude) into consideration. We output sun/rise set times, star rise/set times, star observation logs (altitude, azimuth, conditions), and general survey metadata.

Our radial velocity precision code uses a semi-analytic model of astrophysical sources of uncertainty, given an input SNR and wavelength range (Beatty and Gaudi 2015). This model considers the effects of: Stellar spectrum (BT-Settl), spectrograph resolution, log(g), T_{eff}, metallicity, v·sin(i), and macroturbulence on RV signal. It does not consider stellar activity or tellurics as noise sources.

Instruments are simulated, though not in-depth. Instrument throughput, readout and dark noise, pixel scale, and some atmospheric scattering are considered.

These RV information and noise sources are fed into an exposure time calculator, so that a desired photon noise/precision level can be reached. The exposure time calculator can also be set based on SNR in a given resolution element and/or a fixed minimum exposure. A five minute minimum is used here to compensate for stellar P-mode oscillations.

Acknowledgements

This research is supported by a contract from the NASA Jet Propulsion Laboratory and Exoplanet Exploration Program in support of the HabEx Mission Study Science and Technology Definitions Team.

Planet Recovery (Figure of Merit)

To avoid compute-intensive injection and recovery tests, we use a figure of merit that assumes a planet of arbitrary mass and (aside from being much shorter than the survey duration unknown arbitrary period) in a circular orbit around the star. (Gaudi and Winn 2007)

$$SNR = \frac{K}{\sigma}\sqrt{\frac{N_{\mathrm{obs}}}{2}} \quad (1)$$

Since we consider σ as both photon noise and detector noise (potentially varying between sites in a multi-telescope survey), this is actually a composite value that can vary between observations. Both SNR for a potential k = 10 cm/s, and k for an SNR = 10 detection are considered for all architectures.

Selected Results

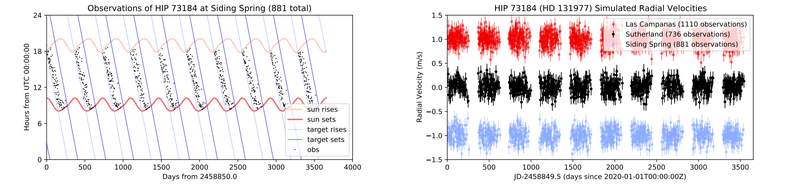

Figure: HIP 73184 (HD 131977) as observed in architecture I. Left: star rise/set, sun rise/set, and observation times over the course of the survey. Right: Radial-velocity timeseries.

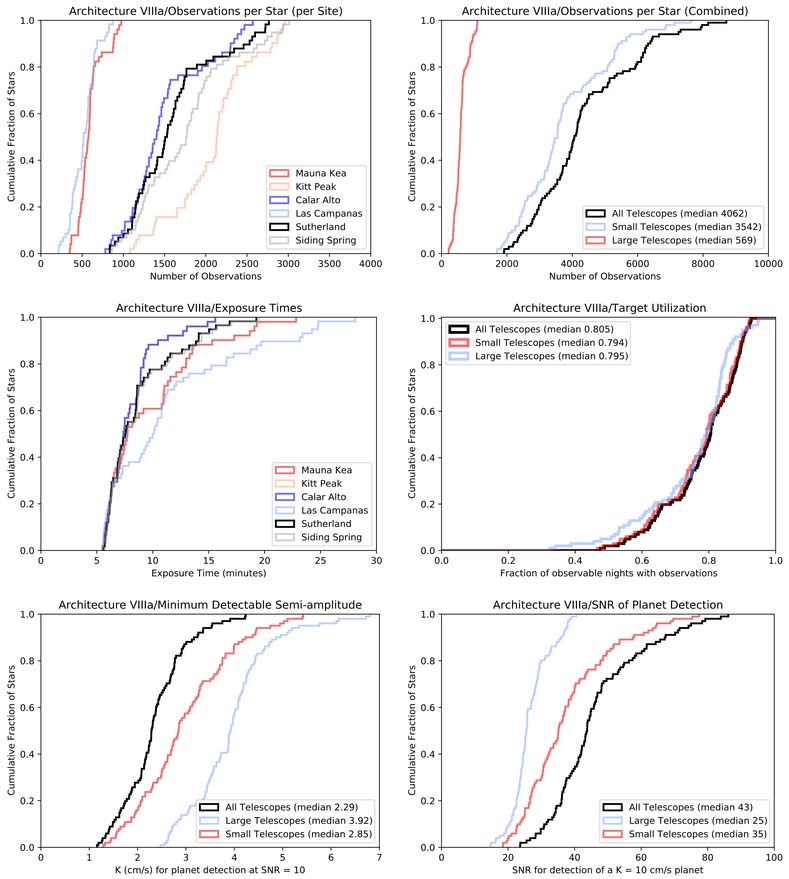

Figure: Cumulative distributions of: observations per star (both per-site and combined), exposure times per star, fraction of nights with good weather each star was observed, minimum semi-amplitude.

Conclusions and Future Work

If single measurement precisions of 10 cm/s can be obtained, then an extended campaign may be able to find earth analogs. Direct analogs around sunlike stars are in a marginal region, but super-earths and cooler stars are distinctly practical.

As for specific instruments, the effect of a given spectrograph design appears less decisive than the telescopes. Six dedicated telescopes with a global distribution can achieve true nightly cadence under a number of circumstances, resulting in a sufficient number of observations to plausibly detect earth-like planets in the habitable zones of sun-like stars both in idealized sensitivity, and with headroom for noise modeling.

We are currently looking into to what extent stellar activity degrades these signals, and how much it can be corrected.

Survey Results

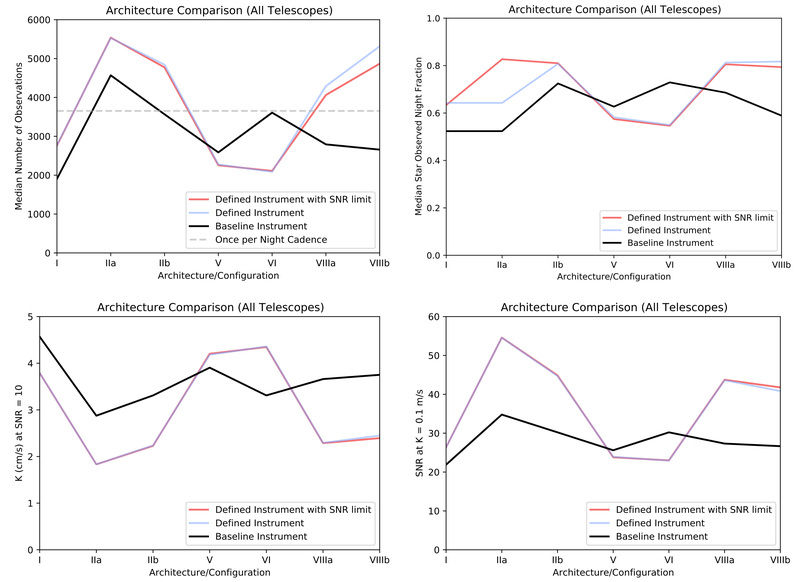

Figure: Comparison of median results across architectures. Here, multiple survey setups are shown: with the architecture-defined instrument and target per-measurement SNR, the architecture-defined instrument without the SNR restriction, and a baseline instrument.

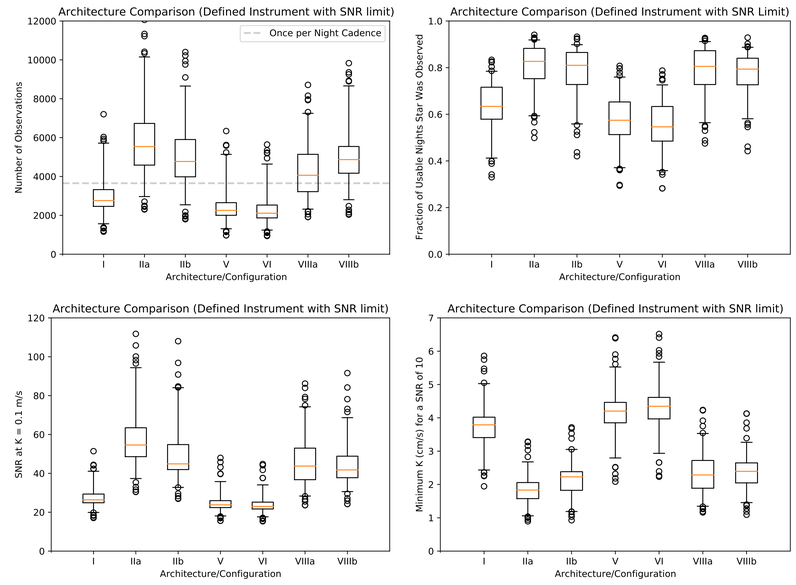

Figure: Comparison of the distribution of number of observations, observation efficiency, and planet detection sensitivity/signal strength. Boxes are at 25/75%, and whiskers at 5/95%.

References

Luhn, Jacob K., et al. (2022) Impact of Correlated Noise on the Mass Precision of Earth-analog Planets in Radial Velocity Surveys. The Astronomical Journal (accepted) https://arxiv.org/abs/2204.12512

Swift et al. (2015). Miniature Exoplanet Radial Velocity Array (MINERVA) I. Design, Commissioning, and First Science Results. J. Astron. Telesc. Instrum. Syst. 1(2), 027002. dx.doi.org/10.1117/1.JATIS.1.2.027002

Beatty, Thomas G. & Gaudi, B. Scott. (2015) Astrophysical Sources of Statistical Uncertainty in Precision Radial Velocities and Their Approximations. Publications of the Astronomical Society of Pacific, 127(958), 1240. dx.doi.org/10.1086/684264

Gaudi, B. Scott., & Winn, Joshua N. (2007) Prospects for the Characterization and Confirmation of Transiting Exoplanets via the Rossiter-McLaughlin Effect. The Astrophysical Journal, 655(1), 550-563.

Crass, Jonathan et al. (2021) Extreme Precision Radial Velocity Working Group Final Report. arXiv e-prints. https://exoplanets.nasa.gov/exep/NNExplore/EPRV/